Interaction of solitons with bond defects in discrete nonlinear Schrödinger chains

M. T. Primatarowa, K. T. Stoychev, and R. S. Kamburova
Institute of Solid State Physics, Bulgarian Academy of Sciences, 1784 Sofia, Bulgaria
(Received 1 February 2008; published 11 June 2008)

The interaction of solitons with bond defects in discrete nonlinear Schrödinger (NLS) chains is investigated. A perturbed NLS equation is derived on the basis of a microscopic model. Localized soliton-defect solutions are obtained and their stability is analyzed. Scattering of propagating solitons from bond defects is studied numerically and a variety of scattering patterns is obtained. A phase diagram is constructed showing the corresponding parametric regions.

DOI: 10.1103/PhysRevE.77.066604 PACS number(s): 05.45.Yv, 63.20.Ry, 63.20.kp, 63.20.Pw

I. INTRODUCTION

The interaction of solitons with defects and inhomogeneities is a problem of continuing interest due to its theoretical and practical importance. Widely investigated is the interaction of solitons with linear and nonlinear point defects [1–11]. The role of modified coupling constants (bond defects) on the soliton dynamics has been studied in a few works [12–15]. Breather trapping in a region of modified coupling constants has been investigated in Ref. [12] for a DNA model. In Ref. [13] an inhomogeneous waveguide array with a modified coupling constant has been considered and a perturbed nonlinear Schrödinger (NLS) equation has been obtained. Localized states in the presence of a power-law nonlocal dispersive interaction has been studied in Ref. [14] including both short-range and long-range interaction. In Ref. [15] low-energy excitations in spin-Peierls chains with modified bonds have been investigated and bound soliton-impurity solutions as a function of the lattice size have been obtained. Interaction of NLS solitons with extended inhomogeneities with modified dispersion coefficients has been studied in Ref. [16] and periodically repeating regions of trapping and transmission have been obtained as a function of the size of the inhomogeneity.

In the present work we investigate in detail the interaction of solitons with modified-bond defects in discrete nonlinear Schrödinger (DNLS) chains. The paper is organized as follows. A NLS equation is derived in Sec. II which includes three perturbing terms associated with the bond defect. Localized soliton-defect solutions are obtained in Sec. III and their stability is analyzed. Scattering of solitons from the bond defects is studied numerically in Sec. IV and a variety of scattering patterns is obtained for different soliton velocities and defect strengths. Section V concludes the investigation.

II. THE PERTURBED NLS EQUATION

We shall investigate the soliton dynamics of nonlinear Bose-type excitations in a discrete chain with a modified exchange interaction (bond defect) between sites 0 and 1. The corresponding Hamiltonian in the nearest-neighbor approximation can be written as

$$H = \omega_0 \sum_n B_n^\dagger B_n + \frac{1}{2}\sum_n (M + \mu\delta_{n,0})(B_{n+1}^\dagger B_n + B_n^\dagger B_{n+1}) + \frac{g}{2}\sum_n B_n^\dagger B_n^\dagger B_n B_n. \quad (1)$$

$B_n^\dagger$ and B_n are the corresponding creation and annihilation operators of excitations at site n, ω_0 is the harmonic on-site energy ($\hbar = 1$), g is the nonlinearity constant, M is the transfer matrix element between neighboring sites in the ideal lattice, and μ describes the modification of the matrix element between sites 0 and 1 (a single bond defect).

The equations of motion for the averaged amplitudes $\alpha_n \equiv \langle B_n \rangle$ yield

$$i\frac{\partial \alpha_n}{\partial t} = \omega_0 \alpha_n + \frac{1}{2}[(M + \mu\delta_{n,0})\alpha_{n+1} + (M + \mu\delta_{n-1,0})\alpha_{n-1}] + g|\alpha_n|^2\alpha_n. \quad (2)$$

We shall look for solutions in the form of amplitude-modulated monochromatic waves

$$\alpha_n(t) = \varphi_n(t)e^{i(kn-\omega t)}, \quad (3)$$

where k and ω are the wave number and the frequency of the carrier wave (the lattice constant equals unity) and the envelope $\varphi_n(t)$ is a real slowly varying function of the position and time. In the continuum limit, Eq. (2) transforms into the following perturbed nonlinear Schrödinger equation for the envelope:

$$i\frac{\partial \varphi}{\partial t} = \{\omega_0 - \omega + [M + \mu\delta(x)]\cos k\}\varphi + i \sin k[M + \mu\delta(x)]\frac{\partial \varphi}{\partial x} + \frac{1}{2}[M + \mu\delta(x)]\cos k\frac{\partial^2 \varphi}{\partial x^2} + g|\varphi|^2\varphi. \quad (4)$$

It is worth discussing here some specific features of bond defects. While linear and nonlinear on-site defects yield single δ-function perturbing terms in the NLS equation, a bond defect introduces three δ-function perturbing terms in Eq. (4). A noteworthy feature of the bond-defect terms is their wave number dependence. As the carrier wave number is related to the soliton velocity, this is essentially a velocity dependence. In Ref. [13] the role of the bond defect has been

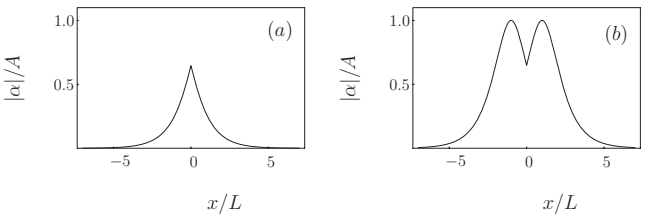

FIG. 1. Bound soliton-defect solution (5) for (a) $\Delta=1$ and (b) $\Delta=-1$.

reduced to a linear point-defect term and in Ref. [12] to a second-derivative perturbing term. Equation (4) includes both these terms in the long wavelength (slow soliton) limit ($k\sim v\ll 1$). However, Eq. (4) includes also a first-derivative term $\sim\mu \sin k\delta(x)$ which plays an important role and can dominate the scattering of fast solitons from bond defects.

III. BOUND SOLITON-DEFECT SOLUTIONS

In the static case $k=v=0$ the terms $\sim\sin k$ vanish and for wide solitons ($L\gg 1$) the term $\delta(x)\partial^2\varphi/\partial x^2$ can be neglected compared to the term $\delta(x)\varphi$ as being L^2 times smaller. In the present work we shall consider only the case $M/g>0$, corresponding to bright solitons. Investigations of the interaction of dark solitons ($M/g<0$) with bond defects will be the subject of another work. Under the above assumptions Eq. (4) possesses the following bound soliton-defect solution:

$$\alpha(x,t)=A\ \mathrm{sech}\left(\frac{|x|}{L}+\Delta\right)e^{-i\omega t} \tag{5}$$

with A, ω, and Δ given by

$$A^2=\frac{M}{gL^2},\quad \omega=\omega_0+M+\frac{M}{2L^2},\quad \Delta=\tanh^{-1}(\mu L/M). \tag{6}$$

For $\Delta>0$ the function $|\alpha(x)|$ has a single maximum at $x=0$ and for $\Delta<0$ the function $|\alpha(x)|$ has two maxima at $x=\pm\Delta L$. Note that Eq. (6) implies $|\mu L/M|\leq 1$, which is the necessary condition for the existence of bound solutions.

Further on we shall consider $M<0$ (positive effective mass) and $g<0$ (attractive nonlinear interaction). $\mu<0$ (increased absolute value of the dispersion coefficient) corresponds to an attractive potential and yields a single-peak solution [Fig. 1(a), $\Delta>0$], while $\mu>0$ (decreased absolute value of the dispersion coefficient) corresponds to a repulsive potential and yields a double-peak solution [Fig. 1(b), $\Delta<0$]. From a classical point of view the double-peak solution can be seen as two particles at equilibrium in the presence of a defect-induced repulsive force, balanced by a nonlinear attractive force.

In what follows we present results of numerical solutions of Eq. (2). In the simulations we used 2000 lattice sites and periodic boundary conditions. The accuracy of the computations was controlled through the conservation of the norm and the energy (the corresponding relative variations were less than 10^{-5} and 10^{-4}, respectively).

It should be pointed out that as follows from Eq. (2), a single bond defect affects the two adjacent sites and hence it

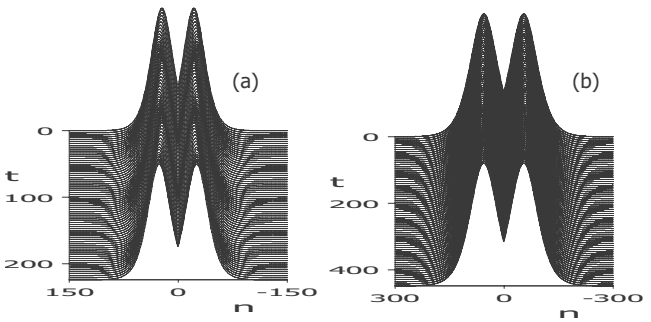

FIG. 2. Evolution of the solution (5) with $M=g=-0.2$ for (a) $L=20$, $\mu=0.008$ and (b) $L=50$, $\mu=0.0032$. The time is measured in units $10^3/\omega_0$.

is effectively larger in size than a single on-site defect. This imposes more severe restrictions on the width of the double-peak bond-defect solutions (5) compared to these for on-site defects. While the latter are stable for $L=10$, bond-defect solutions (5) with $L=10$ are destroyed. For $L=20$ the bond-defect solution exhibits long-lasting shape oscillations [Fig. 2(a)]. We obtained similar shape oscillations when we input two adjacent linear point defects in the equations. This shows unambiguously that the oscillations in Fig. 2(a) are a discreteness-induced effect, which is much stronger in the case of bond defects compared to single on-site defects. We obtained unperturbed localized bond-defect solutions for $L\geq 50$ [Fig. 2(b)].

Next we studied the stability of the bound soliton-defect solutions (5) against different perturbations. Our numerical simulations showed that the single peak solution, which corresponds to an attractive bond defect, remains stable for strong initial perturbations. The double peak solution, however, which results from a delicate balance between a repulsive bond-defect interaction and an attractive nonlinear interaction between the peaks, is very sensitive to perturbations. It should be pointed out that the double-peak solution is stable only if centered in the middle of the defect bond. In our case this is the middle point between sites 0 and 1. Small symmetric initial perturbations, such as wrong input amplitude A' [Fig. 3(a)] or wrong input peak positions Δ' [Fig. 3(b)] induce long-lasting oscillations of the double-peak solution. In both cases the input peak positions differ from their equilibrium positions. Small asymmetric perturbations destroy the double peak solution. On Fig. 3(c) we have shifted the center of the input solution from $n=1/2$ to $n=0$. It is seen that in this case the initial solution splits into two separate solitons with different amplitudes and velocities. Similar behavior of the soliton-defect solutions for linear defects has been observed in Ref. [7].

IV. SCATTERING OF SOLITONS FROM BOND DEFECTS

For a homogeneous chain with $\mu=0$ and $M\cos k/g>0$ Eq. (4) possesses a fundamental bright soliton solution

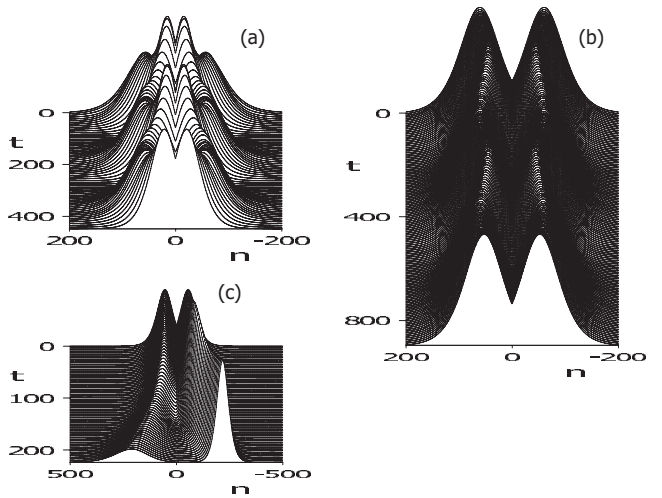

FIG. 3. Stability of the static solution (5) with $L=50$ and $\mu=0.0032$ against initial perturbations: (a) wrong input amplitude $A'=1.1A$, (b) wrong input peak positions $\Delta'=1.1\Delta$, (c) shift of the center of the solution from the center of the defect ($n=0.5$) to $n=0$.

$$\alpha(x,t) = A\ \mathrm{sech}\frac{x-vt}{L}e^{i(kx-\omega t)}, \quad A^2 = \frac{M\cos k}{gL^2},$$

$$v = -M\sin k, \quad \omega = \omega_0 + M\cos k + \frac{M\cos k}{2L^2}. \tag{7}$$

Note that the soliton velocity v within our model is limited to $|M|$. We used the solution (7) as initial condition in the simulations, placed sufficiently apart from the defect. The evolution of the input pulse depends on the initial soliton parameters, the material parameters and the defect strength. In the long-wavelength limit ($k \ll 1, v \approx -Mk$) we can define three different energies: a kinetic energy associated with the soliton velocity E_k, a nonlinear (potential) energy related to the soliton amplitude E_{nl} and energy of interaction of the soliton with the defect $E_d \sim \mu$. For the Hamiltonian (1) and the solution (7), the corresponding energies take the forms

$$E_k = \frac{v^2}{2|M|}N, \quad E_{\mathrm{nl}} = \frac{M}{6L^2}N, \quad \text{and} \quad E_d = \frac{\mu}{2L}N \tag{8}$$

where $N=2LA^2$ is the norm. The interplay between these energies governs the evolution of the soliton pulse. Some general features of the scattering of slow and fast solitons from point defects have been obtained in Ref. [1]. In the case of strong nonlinearity the soliton behaves similar to a particle and it is either transmitted or reflected as a whole with some emitted radiation. In the opposite case of weak nonlinearity, the scattering pattern is similar to this of linear waves, i.e., the initial pulse is split into transmitted and reflected parts governed by the corresponding Fresnel coefficients. Investigation of soliton scattering patterns for different defect strengths has been carried out in Ref. [2] and regions of transmission and trapping have been obtained. In the present work we carried out an extensive numerical study of the

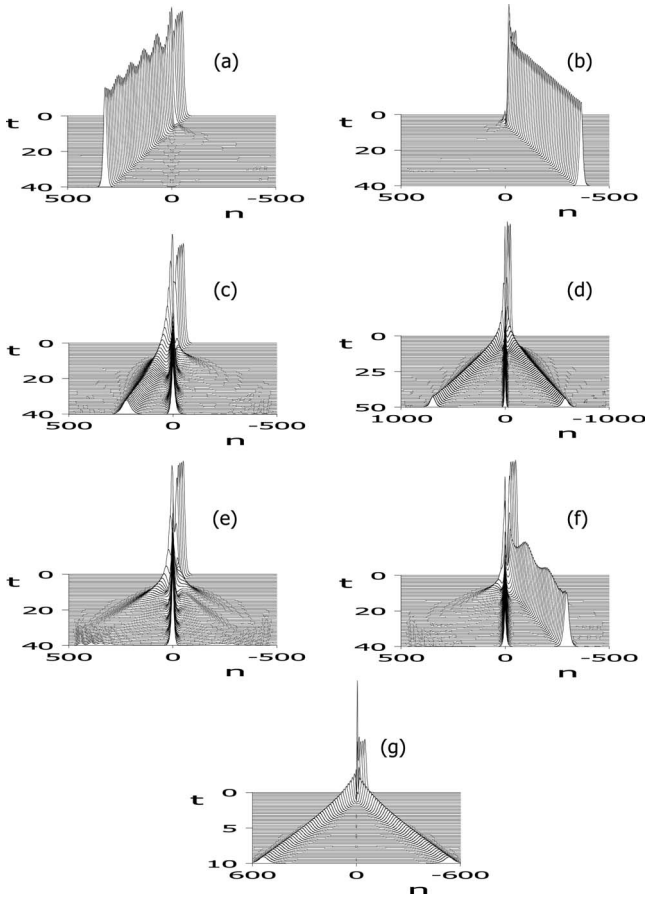

FIG. 4. Scattering of a solitons with $L=10$ from an attractive bond defect. (a) $v=0.01$, $\mu=-0.0028$, (b) $v=0.01$, $\mu=-0.04$, (c) $v=0.01$, $\mu=-0.0064$, (d) $v=0.015$, $\mu=-0.014$, (e) $v=0.01$, $\mu=-0.01$, (f) $v=0.01$, $\mu=-0.016$, (g) $v=0.059$, $\mu=-0.066$.

scattering of solitons from bond defects for a wide range of soliton velocities and defect strengths. Most interesting and rich in evolutionary patterns is the case when $E_k \sim |E_{\mathrm{nl}}| \sim |E_d|$. Typical three-dimensional (3D) plots representing the different types of scattering from attractive bond-defects are presented in Fig. 4. A phase diagram in the $v-\mu$ space, showing the regions corresponding to the different scattering patterns is shown in Fig. 5.

In the case of fast solitons and small defect strengths when $E_k \gg |E_d|$ the soliton is transmitted through the defect with minor perturbations [Fig. 4(a)]. The region corresponding to this type of scattering is marked with (a) on Fig. 5. In the opposite case of slow solitons and large defect strengths, when $E_k \ll |E_d|$, the soliton is reflected by the defect (no matter that the latter is attractive). The corresponding region is marked (b) on Fig. 5 and a typical 3D plot is shown in Fig. 4(b). The wide area between regions (a) and (b) corresponds to $E_k \sim |E_d|$ and involves regions with different outcomes. In the case of slow solitons, an increase of the defect strength above the threshold for transmission leads to splitting of the soliton into a transmitted and a trapped part [Fig. 4(c)]. The corresponding region is marked with (c) on Fig. 5. A further increase of the defect strength for solitons with $(0.01 < v < 0.04)$ yields a region surrounded by dots (d) in which the initial soliton is decomposed into transmitted, reflected, and

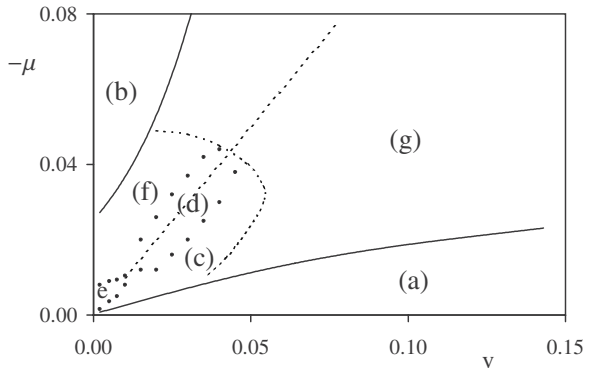

FIG. 5. Regions in the $v-\mu$ space corresponding to the evolutionary patterns in Fig. 4, marked by the same letters for consistency.

trapped parts [Fig. 4(d)]. The transmitted and reflected solitons are wider and with smaller, nearly equal amplitudes, while the trapped part is narrower, with a larger amplitude and corresponds to a nonlinear localized mode. For very slow solitons ($v<0.01$) there exists a region near the origin surrounded by dots (e) where the transmitted and reflected waves decay and only the trapped nonlinear mode remains as an outcome of the scattering process. The corresponding evolutionary pattern is shown in Fig. 4(e). Between regions (d), (e), and (b) lies a region (f) where the incoming soliton splits into reflected and trapped parts [Fig. 4(f)]. The wide region (g) on Fig. 5 situated between regions (a) and (b) for $v\geq 0.04$ corresponds to splitting of the soliton into a transmitted and reflected parts [Fig. 4(g)]. Due to the higher soliton velocity, no trapped state is excited in this case.

The dashed line $v=-\mu$ corresponds to the condition for equal transmission and reflection coefficients for scattering of linear waves from point defects with strength μ. In our case, this line corresponds to transmitted and reflected solitons equal amplitudes. This should not be surprising as in this region $|E_d|\gg|E_{\mathrm{nl}}|$ and the nonlinear term in the NLS equation can be neglected compared to the defect-induced perturbing terms. Thus the scattering of these weakly-nonlinear waves is governed by the conditions for linear waves. For weaker soliton velocities and defect strengths, the nonlinear terms become important, which leads to partial or complete trapping of the soliton on the defect. Our results show that the trapped states occur for soliton and defect parameters near the $v=-\mu$ line. Thus the condition for transmitted and reflected linear wave with equal amplitudes favors trapping of the solitons in the nonlinear case.

V. CONCLUSION

The role of bond defects on the soliton dynamics in DNLS chains is investigated. A nonlinear Schrödinger equation is derived in the continuum limit, which includes three velocity-dependent perturbing terms associated with the defect. Bound soliton-defect solutions are obtained analytically and their stability against initial perturbations is investigated. The single-peak solution which corresponds to an attractive bond-defect potential is extremely stable against perturbations. On the contrary, the double-peak solution corresponding to a repulsive defect potential is unstable and it is easily destroyed by asymmetric perturbations.

Scattering of solitons from bond defects is studied numerically. A rich variety of scattering patterns is obtained in the case of attractive defects and $E_k\sim|E_d|$. A phase diagram is constructed in $v-\mu$ space showing the regions corresponding to the different types of scattering.

ACKNOWLEDGMENTS

This work was supported in part by the National Science Foundation of Bulgaria under Grant No. F1414.

[1] Yu. S. Kivshar, A. M. Kosevich, and O. A. Chubykalo, Zh. Eksp. Teor. Fiz. **93**, 968 (1987); Yu. S. Kivshar, A. M. Kosevich, and O. A. Chubykalo, Phys. Lett. A **125**, 35 (1987); Yu. S. Kivshar, A. M. Kosevich, and O. A. Chubykalo, Sov. Phys. JETP **66**, 545 (1987).
[2] X. D. Cao and B. A. Malomed, Phys. Lett. A **206**, 177 (1995).
[3] K. Forinash, M. Peyrard, and B. Malomed, Phys. Rev. E **49**, 3400 (1994).
[4] V. V. Konotop, D. Cai, M. Salerno, A. R. Bishop, and N. Grønbech-Jensen, Phys. Rev. E **53**, 6476 (1996).
[5] D. I. Pushkarov and R. D. Atanasov, Phys. Lett. A **149**, 287 (1990).
[6] Yu. S. Kivshar, Phys. Lett. A **161**, 80 (1991).
[7] A. D. Boardman, V. Bortolani, R. F. Wallis, K. Xie, and H. M. Mehta, Phys. Rev. B **52**, 12736 (1995).
[8] S. Burtsev, D. J. Kaup, and B. A. Malomed, Phys. Rev. E **52**, 4474 (1995).
[9] A. A. Sukhorukov, Yu. S. Kivshar, O. Bang, J. J. Rasmussen, and P. L. Christiansen, Phys. Rev. E **63**, 036601 (2001).
[10] P. G. Kevrekidis, Yu. S. Kivshar, and A. S. Kovalev, Phys. Rev. E **67**, 046604 (2003).
[11] M. T. Primatarowa, K. T. Stoychev, R. S. Kamburova, and J. Optoel, Adv. Math. **9**, 152 (2007).
[12] J. J.-L. Ting and M. Peyrard, Phys. Rev. E **53**, 1011 (1996).
[13] W. Królikowski and Yu. S. Kivshar, J. Opt. Soc. Am. B **13**, 876 (1996).
[14] K. Ø. Rasmussen, P. L. Christiansen, M. Johansson, Yu. B. Gaididei, and S. F. Mingaleev, Physica D. **113**, 134 (1998).
[15] D. Augier, J. Riera, and D. Poilblanc, Phys. Rev. B **61**, 6741 (2000).
[16] K.T. Stoychev, M.T. Primatarowa, and R.S. Kamburova, Phys. Rev. E **73**, 066611 (2006).